

**THE CATALYTIC MECHANISM OF HUMAN  
SERINE/THREONINE PROTEIN PHOSPHATASE 2C $\alpha$**

by  
Clark Charles Fjeld

A Thesis

Presented to the Department of Biochemistry and Molecular Biology  
and to the Oregon Health Sciences University  
School of Medicine  
in partial fulfillment of  
the requirements for the degree of  
Master of Science  
April 1999

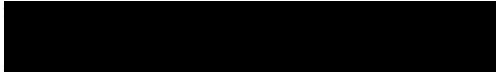
School of Medicine  
Oregon Health Sciences University

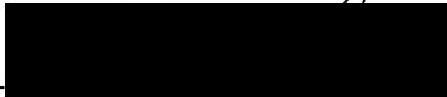
---

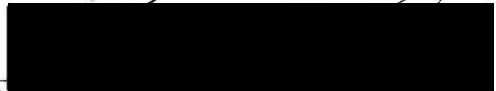
CERTIFICATE OF APPROVAL

---


This is to certify that the M.S. thesis of  
Clark Charles Fjeld  
has been approved


  
\_\_\_\_\_  
Professor in charge of thesis

  
\_\_\_\_\_  
Member

  
\_\_\_\_\_  
Member

  
\_\_\_\_\_  
Member

  
\_\_\_\_\_  
Member

  
\_\_\_\_\_  
Associate Dean for Graduate Studies

## TABLE OF CONTENTS

	<u>Page</u>
ACKNOWLEDGMENTS	ii
ABSTRACT	iii
ABBREVIATIONS	v
LIST OF FIGURES	vi
CHAPTER	
I        Introduction	1
II       Experimental Procedures	5
III      Results	11
IV      Discussion	16
V       Tables	21
VI      Scheme	24
VII     Figures	25
IX      Summary and Conclusions	37
X       References	38

## ACKNOWLEDGMENTS

I thank Dr. John M. Denu for providing me with a remarkable enzyme to study and for teaching me many powerful tools of enzymology. Dr. Denu's sound experimental approach, keen sense of which questions should be addressed first and unyielding determination to complete the task at hand are qualities that I have witnessed and hopefully acquired.

I thank Dr. Kirk G. Tanner for many helpful discussions fueled by his understanding and genuine interest in the chemistry of biological molecules.

I thank Dr. Jack H. Kaplan for increasing my interest in the unique functionality and reactivity of protein residues as related to protein structure. I thank Dr. Dick G. Brennan for expanding my appreciation for protein structural motifs and how they can be shared by otherwise unrelated proteins. I am fortunate to have learned these concepts from researchers who use them on a daily basis.

## ABSTRACT

The serine/threonine protein phosphatase 2C $\alpha$ , is a Mn<sup>+2</sup>- or Mg<sup>+2</sup>- dependent enzyme that plays a major role in downregulating stress response in bacteria, plants, yeast and mammals. The X-ray structure has been solved for this enzyme containing a phosphate molecule bound proximal to a dinuclear metal cation site which is sandwiched between two  $\beta$ -sheets suggesting the location of the active site. A catalytic mechanism has been proposed based on this structural information involving a nucleophilic, metal-activated water molecule which hydrolyzes the phosphomonoester bond in a one step reaction. Little experimental evidence is available to corroborate or contest this proposal. Thus, we have set out to elucidate the catalytic mechanism of human protein phosphatase 2C $\alpha$  using steady-state and pre-steady-state kinetics.

A detailed investigation of the catalytic mechanism of protein phosphatase 2C $\alpha$  has been carried out using bisubstrate, product inhibition and leaving group dependence studies. The bisubstrate studies demonstrated that the enzyme utilizes a sequential mechanism and the formation of a ternary-complex is required for catalysis. Product inhibition analysis suggested an ordered mechanism where divalent cations bind prior to phospho-substrate and where the alcohol product is released before phosphate. Determination of Brönsted values at pH 7.0 and 8.5 using several phosphorylated substrates differing by the pK<sub>a</sub> of the leaving group, suggested a pH dependent rate limiting step with chemistry being rate limiting at the lower pH value and some other step, such as phosphate release, being rate limiting at the higher pH value. The results of pre-steady-state experiments supported a catalytic scheme where the slow step at pH 8.5 occurs after release of the alcohol product and is common among the various substrates analyzed in the Brönsted plots. It is likely that the rate limiting step at higher pH is phosphate release.

Analysis of the enzyme's pH dependence revealed a group that must be unprotonated for catalysis in both the  $k_{cat}$  and  $k_{cat}/K_m$  pH profiles with a pK<sub>a</sub> value of 7.0

and 7.2, respectively. The enzyme also requires that a group with a  $pK_a$  value of 9.0 to be protonated for substrate binding as determined in the  $k_{cat}/K_m$  pH profile. The ionization which must be unprotonated and has a  $pK_a$  value of 7.0 is likely to be an activated water molecule proposed to be the nucleophile.

The substrate specificity of the enzyme was probed using several phosphorylated peptides and the metal cation specificity was explored using several divalent cations. The  $k_{cat}/K_m$  values obtained revealed that diphosphorylated peptides with neighboring phosphorylation sites were preferred substrates over peptides singly phosphorylated on threonine residues. This result is in agreement with the recent findings that several diphosphorylated proteins are substrates of protein phosphatase 2C $\alpha$ . The  $k_{cat}/K_m$  for the divalent cations revealed that  $Fe^{+2}$  is preferred over all other divalent cations tested. This observation is of interest considering that this phosphatase is defined as a  $Mn^{+2}$ - or  $Mg^{+2}$ -dependent enzyme.

## Abbreviations

The abbreviations used are: MAPK, mitogen-activated protein kinase; MAPKK, MAPK kinase; MAPKKK, MAPKK kinase; PP2C $\alpha$ , Protein Phosphatase 2C $\alpha$ ; PP1, Protein Phosphatase 1; PP2A, Protein Phosphatase 2A; PP2B, Protein Phosphatase 2B; PTP1, Protein Tyrosine Phosphatase 1; M1, metal-binding site 1; M2, metal-binding site 2; *p*NPP, *para*-nitrophenylphosphate; *p*-NP, *para*-nitrophenol; EDTA, ethylenediamine-tetraacetic acid; ferrozine, 3-(2-pyridyl)-5,6-bis(4-phenylsulfonic acid)-1,2,4-triazine; IPTG, isopropyl- $\beta$ -D-thiogalactopyranoside; DTT, dithiothreitol; EGTA, [ethylene-bis(oxyethylenitrilo)]tetraacetic acid; PMSF, phenylmethylsulfonyl fluoride; Bis-Tris, (bis[2-hydroxyethyl]imino-tris[hydroxymethyl]methane; DiFUMBP, 6,8-difluoro-4-methylumbelliferyl phosphate;  $\epsilon$ , molar extinction coefficient.

## LIST OF FIGURES

<u>Figure</u>	<u>Page</u>
1      Saturation kinetics of PP2C with $\text{Mn}^{+2}$ .	25
2      Oxidation of $\text{Fe}^{+2}$ correlates with loss in PP2C activity.	26
3A     Effect of pH on the $k_{\text{cat}}$ parameter at saturating $\text{Mn}^{+2}$ .	27
3B     Effect of pH on the $k_{\text{cat}}/K_m$ parameter at saturating $\text{Mn}^{+2}$ .	28
4A     Effect of pH on the $k_{\text{cat}}$ parameter at saturating $\text{Mg}^{+2}$ .	29
4B     Effect of pH on the $k_{\text{cat}}/K_{p\text{NPP}}$ parameter at saturating $\text{Mg}^{+2}$ .	30
5      Ternary-complex mechanism of PP2C $\alpha$ .	31
6A     Phosphate inhibition of PP2C at varied $p\text{NPP}$ .	32
6B     Phosphate inhibition of PP2C at varied metal.	33
7      Effect of leaving group $\text{pK}_a$ value on the $k_{\text{cat}}$ .	34
8A     Pre-steady state analysis reveals product “burst.”	35
8B     Burst amplitude is dependent on enzyme concentration.	36



## INTRODUCTION

Protein phosphatases (PP) catalyze the dephosphorylation of proteins containing phosphoserine/phosphothreonine and are divided into two distinct gene families, designated PPP and PPM (1). Although both PP families require divalent cations for activity, the PPM family is often distinguished by its  $Mg^{+2}$ - and  $Mn^{+2}$ -dependence. PP2C is the defining member of the PPM family. PP2C homologues have been identified in bacteria, plants, yeast and mammals and appear to have a conserved role in negatively regulating stress response. PP2C has been shown to be a negative regulator of the two mitogen-activated protein kinase (MAPK) pathways involved in stress response, the p38 and c-Jun N-terminal kinase (JNK) pathways. Like other MAPK pathways, these consist of a MAPK, a MAPK kinase (MAPKK) and a MAPKK kinase (MAPKKK) (2). The MAPK is phosphorylated on conserved threonine and tyrosine residues by the activated MAPKK. The MAPKK is activated by phosphorylation on conserved threonine and/or serine residues by the MAPKKK.

PP2C is thought to directly dephosphorylate and inactivate protein kinases at several points in the cascade. The stress response pathways are activated by proinflammatory cytokines as well as cellular stresses such as osmotic shock, oxidative stress, UV irradiation and heat shock (3, 4). The PP2C homologue, MP2C, functions as a negative regulator of a stress-activated pathway in plants. By a yeast genetic analysis, the molecular target of MP2C was determined to be the MAPKKK Ste11, suppressing the MAPK pathway (5). MKK6 and SEK 1, both MAPKKs important in stress response signaling pathways, have been identified as PP2C substrates (6). Additional MAPKKs have also been suggested to be PP2C substrates (7). PP2C $\alpha$  has been shown to dephosphorylate and inactivate the MAPK p38 (6). Genetic studies with PP2C yeast homologues Ptc1, Ptc2 and Ptc3 (8, 9) indicated that PP2C plays an essential role in downregulating the stress response downstream to the MAPK cascade. Collectively, these studies demonstrate a major role for PP2C in turning off, or resetting, the stress response

pathways. Unlike the PPP family of protein phosphatases, there are no known specific inhibitors of PP2C and no regulatory subunits have been identified. The catalytic domain appears to be sufficient to impart strict substrate specificity.

The crystal structure of monomeric, human PP2C $\alpha$  (~43 kD) bound with Mn<sup>+2</sup> has been solved (10) and reveals a central  $\beta$ -sandwich surrounded by  $\alpha$ -helices. The active site is located at one end of this  $\beta$ -sandwich and is composed of several invariant carboxylates which serve as metal-coordinating residues. There are two hexa-coordinated metal sites, M1 and M2, which are 4 Å apart and share a water molecule and the carboxylate side chain of Asp-60. Site M1 is coordinated by 3 water molecules and two additional aspartic acids, Asp-239 and Asp-282. Site M2 is coordinated by 4 water molecules and makes only two direct contacts with the protein, at the backbone carbonyl of Gly-61 and at the bridging Asp-60. The presence of a bound phosphate in the X-ray structure suggests the importance of an active site arginine. This arginine appears to position the phosphate near the water molecule bridged by the two metal ions. Das *et al.* (10) have suggested that catalysis proceeds by direct attack of an activated water molecule at the phosphorus center of the substrate. Except for this crystallographic study, very little mechanistic data is available for this important class of enzymes.

Structural similarities between PP2C, PP1 and calcineurin coupled to the following mechanistic studies led to the proposal that a water molecule and not a protein residue is the nucleophile with PP2C: 1) the failure to monitor a phosphate-water exchange reaction with PP2B (11) and 2) the find that structurally related purple acid phosphatase transfers the phosphogroup with overall inversion of the configuration at phosphorus (12). These data support a one step mechanism involving the direct attack of a water molecule and argues against a protein residue functioning as the nucleophile. Conflicting results with purple acid phosphatase from bovine spleen do exist (13) and suggest that purple acid phosphatase does utilize a covalent enzyme intermediate. The catalytic mechanism of the PPP family is not fully characterized and many questions remain. Critical differences in

active site residues and the overall lack of sequence identity between these two families suggest that the two families may undergo different catalytic mechanisms.

Considering that the crystals were grown at pH 5.0 (10), and our observation that the pH optimum is close to 8.0, it seems likely that the ionization state of residues with  $pK_a$  values sensitive to change in this pH range, would be altered. For example, there are two histidines, His 40 and His 62 which are near the active site and highly conserved. These His residues have no suggested role based on the crystallographic data. It is possible that a pH change from 5.0 to 8.0 would significantly alter the ionization state, and perhaps the functionality, of these residues. The many carboxylates in the active site which appear to be important for metal binding may undergo a significant change in ionization state as a result of a such a pH change. Glu-37 and Asp-38 are designated as metal binding residues. They actually coordinate the metal ion at the M2 site via water molecules. This suggests that they do not bind the metal ion tightly. It is possible that they may have a role in catalysis beyond metal coordination. Perhaps these carboxylates are acting as general acids (i.e. protonating the leaving group) or general bases (i.e. deprotonating the nucleophile). There is also the possibility that a protein residue is the nucleophile similar to the Cys in protein tyrosine phosphatases (PTPs) (14), the Ser in alkaline phosphatase (15) or the His in acid phosphatase (16).

A detailed biochemical analysis of human PP2C $\alpha$  was carried out to elucidate the kinetic and chemical mechanism for the PP2C family of enzymes. Brönsted plots revealed a pH-dependent rate limiting step, where at pH 7.0, chemistry is rate limiting and at pH 8.5, phosphate release is likely rate limiting. An exponential “burst” of product in pre-steady-state kinetic experiments at the high pH is consistent with our model. Bisubstrate studies coupled with product inhibition studies were used to determine that PP2C utilizes an ordered sequential mechanism and to identify the order of substrate binding and product release. The pH-dependence of PP2C activity was analyzed and revealed an ionizable group that must be unprotonated ( $pK_a$  7) and an ionizable group that must be protonated

( $pK_a$  9) for activity. The metal-dependence of PP2C was explored by determining the kinetic parameters,  $k_{cat}$ , and  $k_{cat}/K_m$  for several divalent cations including  $Mg^{+2}$ ,  $Mn^{+2}$  and  $Fe^{+2}$ . The specificity constant,  $k_{cat}/K_m$ , was determined for several phosphorylated peptides and demonstrates that PP2C prefers diphosphorylated substrates which is consistent with the physiological role of PP2C in dephosphorylating the diphosphorylated MAPKKs and p38.

## Experimental Procedures

### *Materials.*

All chemicals were of the highest purity commercially available. Peptides were from the University of Michigan Protein Core facility. The  $\text{Fe}^{+2}$  chelator, 3-(2-pyridyl)-5,6-bis(4-phenylsulfonic acid)-1,2,4-triazine (ferrozine), was obtained from Sigma.

### *Overexpression and Purification of Human PP2C $\alpha$ .*

The plasmid pCW-PP2C $\alpha$  was a generous gift from Dr. Patricia T.W. Cohen (Dundee, University). The enzyme was purified according to the method described (17) with several modifications. The pCW-PP2C $\alpha$  plasmid was used to transform competent BL21/DE3 bacteria. The transformed bacteria were grown on 2xYT plates containing 100  $\mu\text{g}/\text{mL}$  ampicillin. Overnight 10-mL cultures originating from isolated colonies were used to inoculate 1 liter of 2xYT containing 140 mg/liter ampicillin. When the growth reached an optical density of 0.8 at 600 nm, isopropyl- $\beta$ -D-thiogalactopyranoside (IPTG) was added at 100 mg/liter, and the bacteria were grown for an additional 10 h. The cells were harvested by centrifugation at 5,000 x g (15 min), resuspended in 30 mL of buffer A (50 mM Tris-HCl pH 7.5, 1 mM DTT, 1 mM EDTA, 0.1 mM EGTA, 100 mM NaCl, 2 mM  $\text{MnCl}_2$ , 1 mM benzamidine, 0.1 mM PMSF, 0.03% (v/v) Brij-35) and lysed by french press. The cell debris was pelleted by centrifugation at 48,000 x g (20 min), the supernatant decanted, and the protein precipitated between 30% and 55% saturation with  $(\text{NH}_4)_2\text{SO}_4$ . The pellet was resuspended in 8 mL of buffer B (20 mM triethanolamine pH 7.0, 1 mM EGTA, 2 mM  $\text{MnCl}_2$ , 0.1% (v/v)  $\beta$ -mercaptoethanol, 5% (v/v) glycerol, 0.03% (v/v) Brij-35) and dialyzed against 1 liter of buffer B for at least 2 h with one change in buffer. The dialysate was loaded onto a 50 mL Q-Sepharose (Sigma) anion exchange column pre-equilibrated with buffer B. The column was then washed with 250 mL of buffer B and the enzyme was eluted with a 0-0.4 M linear NaCl gradient of 400 mL.

PP2C $\alpha$  elutes at 250 mM NaCl. Fractions containing high phosphatase activity with *para*-nitrophenylphosphate (*p*NPP) were pooled and concentrated to between 5-10 mL by filtration (Centricon 10 Concentrator by Amicon). The concentrated solution was dialyzed against 1 liter of buffer containing 25 mM Na<sub>2</sub>HPO<sub>4</sub> pH 7.0, 1 M (NH<sub>4</sub>)<sub>2</sub>SO<sub>4</sub>, 1 mM DTT, and 2 mM EDTA for at least 1 h with one change of buffer and then loaded onto a 50 mL Phenyl-Sepharose (Sigma) hydrophobic column. The column was then washed with 250 mL of this buffer and eluted with a 1-0 M linear (NH<sub>4</sub>)<sub>2</sub>SO<sub>4</sub> gradient of 400 mL. PP2C $\alpha$  elutes at 200 mM (NH<sub>4</sub>)<sub>2</sub>SO<sub>4</sub>. Fractions with phosphatase activity were analyzed by SDS-polyacrylamide gel electrophoresis (SDS-PAGE) to determine purity. Fractions of highest purity were pooled and concentrated by filtration to a final concentration of 0.04 to 0.4 mM. PP2C $\alpha$  was dialyzed against 1 liter of 50 mM Tris-HCl pH 7.0, 10% (v/v) glycerol, 1 mM DTT, 2 mM EDTA for 2 h with a change after 1 h, followed by a final dialysis in 50 mM Tris-HCl pH 7.0, 10% (v/v) glycerol, 1 mM DTT for 2 h with one change. The EDTA was included to obtain metal free (apo) PP2C. The enzyme was stored at -20 °C or -80 °C until use.

### *Enzyme Kinetics.*

All assays were carried out in a reaction buffer containing 0.05 M Tris, 0.05 M Bis-Tris, and 0.1 M acetate at 25 °C, pH 5-10.3. To determine the kinetic parameters  $k_{cat}$  and  $k_{cat}/K_m$ , the initial velocities were measured at various substrate concentrations, and the data were fitted to Eq. 1. The computer program KinetAsyst (IntelliKinetics, State College, PA.) was used for fitting kinetic data to Eqs. 1 - 7. Three types of assays were used to monitor PP2C phosphatase activity and are described below.

Continuous assay. The continuous assay monitoring the dephosphorylation of *p*NPP was performed using a temperature-controlled Shimadzu *BioSpec-1601* UV-VISIBLE spectrophotometer and monitoring the absorbance change recorded at 410 nm, pH 7.0.

Initial linear rates were determined using the molar extinction coefficient ( $\epsilon$ ) of  $9 \text{ mM}^{-1} \text{ cm}^{-1}$  for the product *para*-nitrophenol (*p*NP) at pH 7.0.

Endpoint assays. Two endpoint assays were also used to measure PP2C activity. The phosphate detection assay was used for measuring the initial linear rates of dephosphorylation of peptides, amino acids and aryl substrates. The release of phosphate was determined using the colorimetric method described by Brothier *et al.* (18) which measures the formation of phosphomolybdate complexes at 850 nm. Briefly, reaction mixtures of 600  $\mu\text{L}$  were stopped with 1 mL 0.5 N HCl containing 30 mg ascorbic acid, 5 mg ammoniumheptamolybdate and 10 mg SDS. For color development, 1.5 mL containing 30 mg sodium arsenite, 30 mg sodium citrate and 30  $\mu\text{L}$  glacial acetic acid were added and the absorbance was read at 850 nm. The other endpoint assay was developed to determine the rate of *p*NPP hydrolysis for the pH profile using the molar extinction coefficient of  $18 \text{ mM}^{-1} \text{ cm}^{-1}$  for *p*NP at basic pH values. This assay was developed after the described (19) method which utilizes a stop solution containing 1 N NaOH. To prevent the precipitation of metal which occurs upon the addition of 1 N NaOH to a PP2C reaction mixture, a stop solution containing 0.5 M EDTA pH 10 was used. A comparison of the continuous assay and the two endpoint assays revealed that these three assays yielded identical rates.

$$v = (k_{\text{cat}} \cdot S) / (K_m + S) \quad [1]$$

#### *Metal Dependence.*

Various concentrations of metal ions were combined with apo PP2C and allowed to incubate for two minutes. The phosphatase reaction was initiated by the addition of *p*NPP to a final concentration of 20 mM and activity was measured using the continuous assay. The inhibition constants for  $\text{Ca}^{+2}$  and  $\text{Zn}^{+2}$  were determined by adding various amounts of  $\text{Mn}^{+2}$  at fixed concentrations of the inhibiting metal ion at saturating levels of *p*NPP. The data were fitted to Eq. 2. to yield the inhibition constant. The inhibition was competitive with respect to  $\text{Mn}^{+2}$ .

$$v = (k_{\text{cat}} \bullet S) / [K_m \bullet (1 + I/K_{is}) + S], \quad [2]$$

where I is the inhibitor concentration and S is the  $\text{Mn}^{+2}$  concentration and  $K_{is}$  is the inhibition constant.

#### *Fe<sup>+2</sup> Detection.*

A reaction mixture containing 3 mM  $\text{Fe}^{+2}$ , 4 mM pNPP and PP2C was separated into two cuvettes. One was monitored for phosphatase activity using the continuous assay and the other was used to monitor the  $\text{Fe}^{+2}$  concentration during the course of the reaction. The  $\text{Fe}^{+2}$  concentration was determined using the  $\text{Fe}^{+2}$  specific chelator, ferrozine, which has a characteristic absorbance at 562 nm. The measured  $\text{Fe}^{+2}$  concentrations and PP2C activity were plotted versus time using the computer program Kaleidagraph (Abelbeck Software).

#### *Steady-state Kinetics.*

The endpoint assay using the EDTA stop solution was used to measure the pH-dependence of PP2C activity. For the construction of the pH profiles,  $k_{\text{cat}}$  and  $k_{\text{cat}}/K_{\text{pNPP}}$  were obtained at various pH values with pNPP as the varied substrate at saturating levels of  $\text{Mn}^{+2}$  (10 mM) or  $\text{Mg}^{+2}$  (40 mM). The pH data for  $\text{Mn}^{+2}$  and  $\text{Mg}^{+2}$  were fitted to Eqs. 3 and 4, respectively, where C is the pH-independent value of either  $k_{\text{cat}}$  or  $k_{\text{cat}}/K_{\text{pNPP}}$ ; H is the proton concentration; and  $K_a$  and  $K_b$  are the ionization constants of the groups involved in the reaction.

$$v = C / (1 + H/K_a) \quad [3]$$

$$v = C / (1 + H/K_a + K_b/H) \quad [4]$$

The catalytic mechanism of PP2C was determined by performing bisubstrate studies treating the metal cation as a pseudo substrate. Continuous assays were performed



by varying the amounts of *p*NPP at fixed levels of  $Mn^{+2}$  and the data were fitted to Eq. 5 where  $K_a$  and  $K_b$  are the Michaelis constants for *p*NPP and  $Mn^{+2}$ , respectively.

$$v = [k_{cat} \cdot A \cdot B / (K_{ia} \cdot K_b + K_a \cdot B + K_b \cdot A + A \cdot B)] \quad [5]$$

The  $P_i$  product inhibition of PP2C was analyzed with  $Mg^{+2}$  to avoid the precipitation of  $Mn^{+2}$  and  $P_i$ . Continuous assays were performed by varying  $Mg^{+2}$  or *p*NPP in saturating levels of the other substrate at fixed concentrations of the product  $P_i$ . The inhibition of  $P_i$  with respect to *p*NPP, was competitive and the data were fitted to Eq. 2; whereas the inhibition of  $P_i$  with respect to metal, was uncompetitive and the data were fitted to Eq. 6.

$$v = [k_{cat} \cdot S / (K_m + S \cdot (1 + I/K_{ii}))] \quad [6]$$

The leaving group dependence of PP2C was analyzed by determining the dephosphorylation rate of several artificial compounds which differ by the  $pK_a$  of the leaving group. Substrates 6,8-difluoro-4-methylumbelliferyl phosphate (DiFUMBP) ( $pK_a = 4.9$ ), *p*NPP (7.1), 4-methylumbelliferyl phosphate (7.8),  $\beta$ -naphthyl phosphate (9.38), phenyl phosphate (9.99), phosphoserine (13) (20) and phosphothreonine in the peptide GIPIRVY(pT)HEV (14.2) (20) were analyzed using the phosphate detection assay at pH 7.0 and 8.5. Brönsted values were obtained by linear least-squares fitting of  $\log(k_{cat})$  versus  $pK_a$  of leaving group for the substrates using the computer program KaleidaGraph (Abelbeck Software.)

### *Pre-steady-state Kinetics.*

Enzyme and substrate were rapidly mixed at pH 8.5 and 25 °C in a temperature-controlled SF-61 stopped-flow spectrophotometer (Hi-Tech Scientific). The absorbance of *p*NP and DiFUMB were monitored at 410 nm and 358 nm, respectively. The enzyme was combined with  $Mn^{+2}$  in the reaction buffer pH 8.5, prior to the rapid mixing with the substrate also diluted into reaction buffer pH 8.5. The final concentration of  $Mn^{+2}$  was 10 mM. The data were fitted to Eq. 7 using the nonlinear least-squares fitting capability of the kinetics software (KinetAsyst, Hi-Tech Ltd, Salisbury, U.K.) where  $A$  is the amplitude of the burst,  $k$  is the first-order rate of the burst,  $B$  is the slope of the linear portion of the curve,  $C$  is the intercept of the line, and  $t$  is time.

$$\text{Absorbance} = A \bullet e^{(-kt)} + B \bullet t + C \quad [7]$$

The amplitude was converted to concentration of *p*NP using the  $\epsilon_{410}$  of 18 mM<sup>-1</sup>cm<sup>-1</sup>. The correlation between the concentration of *p*NP burst and the final enzyme concentration was determined by linear least-squares fitting.

### *Analysis of Peptide Substrates.*

The following phosphopeptides were analyzed as PP2C substrates using the phosphate detection assay: GIPIRVYpTHEV corresponding to Cdc2 kinase (21); KIGEGpTpYGVVYK corresponding to Cdc2 kinase (21) DDE(Nle)pTGpYVATR, corresponding to p38 kinase (22) F(Nle)(Nle)pYPpTVVTR corresponds to JNK kinase with variations of the native -pTPpY- sequence (23). The hydrolysis of phosphotyrosine peptide KIGEGTpYGVVYK was monitored at 282 nm and protein tyrosine phosphatase 1(PTP1) was employed as the positive assay control. Dephosphorylation rates were determined in 10 mM  $Mn^{+2}$  at various peptide concentrations, pH 7.0 and 25 °C.

## Results

### *Metal Dependence.*

The nature of the metal cation has been suggested to be important for regulating the activity of PP2C (24). To explore which divalent cations are effective in activating PP2C,  $k_{\text{cat}}$  and  $k_{\text{cat}}/K_m$  values were determined for several divalent cations at saturating *p*NPP concentrations. The  $k_{\text{cat}}$  constant is the first-order rate constant and reflects the rate-determining step in the overall reaction. The  $k_{\text{cat}}$  reveals the maximal turnover rate of substrate in saturating levels of the metal ion being analyzed. The  $k_{\text{cat}}/K_m$  is the apparent second-order rate constant for the reaction between free enzyme and free substrate and includes the binding of substrate through the first irreversible step. The  $k_{\text{cat}}/K_{\text{metal}}$  parameter reveals the specificity of PP2C and suggests which metal ions are preferred for catalysis. The fact that the metal ion concentration obeys Michaelis-Menten saturation kinetics

(Figure 1), suggests that the metal ions are acting as pseudo-substrates.

Although PP2C has been defined by its  $\text{Mg}^{+2}$ - and  $\text{Mn}^{+2}$ -dependence, these two metals do not activate PP2C to the same extent. A 20-fold higher  $k_{\text{cat}}$  value and 370-fold higher  $k_{\text{cat}}/K_m$  value were observed with  $\text{Mn}^{+2}$  compared to  $\text{Mg}^{+2}$  (Table 1). Surprisingly,  $\text{Fe}^{+2}$  resulted in the greatest activity of all metal ions analyzed, with a 500-fold higher  $k_{\text{cat}}$  value and a 1,800-fold greater  $k_{\text{cat}}/K_{\text{metal}}$  value compared to  $\text{Mg}^{+2}$ . A 7-fold higher  $k_{\text{cat}}$  value and 20-fold greater  $k_{\text{cat}}/K_{\text{metal}}$  value were observed with  $\text{Co}^{+2}$ , as compared to  $\text{Mg}^{+2}$ . A  $k_{\text{cat}}$  value was not determined with  $\text{Cu}^{+2}$  due to precipitation at  $\text{Cu}^{+2}$  levels below enzyme saturation; however, at low concentrations of  $\text{Cu}^{+2}$ , the  $k_{\text{cat}}/K_{\text{metal}}$  was determined by calculating the slope of the initial rate vs. low  $\text{Cu}^{+2}$  concentrations. When PP2C activity was measured with  $\text{Ni}^{+2}$ , the  $k_{\text{cat}}$  and  $k_{\text{cat}}/K_{\text{metal}}$  values were 6-fold lower than those obtained with  $\text{Mg}^{+2}$ . No activity was detected with  $\text{Ca}^{+2}$  or  $\text{Zn}^{+2}$ . These ions were found to competitively inhibit the PP2C  $\text{Mn}^{+2}$ -dependent activity. By varying the  $\text{Mn}^{+2}$

concentration at fixed levels of either  $\text{Ca}^{+2}$  or  $\text{Zn}^{+2}$ , a fit to Eq. 2 yielded  $K_i$  values of  $4.45 \pm 0.54$  mM and  $12.0 \pm 1.8$   $\mu\text{M}$  for  $\text{Ca}^{+2}$  and  $\text{Zn}^{+2}$ , respectively.

To determine the oxidation state of Fe required for PP2C activity, the  $\text{Fe}^{+2}$  detector ferrozine, was used to monitor the effective concentration of  $\text{Fe}^{+2}$  in the phosphatase assay. PP2C activity in a parallel reaction was recorded at specific time points and related to the free  $\text{Fe}^{+2}$  concentration (Figure 2). A direct relationship between loss in  $\text{Fe}^{+2}$  cation (due to oxidation to  $\text{Fe}^{+3}$ ) and loss in activity was observed.

### *pH profiles.*

To determine the ionizations important for catalysis and substrate binding, the  $k_{\text{cat}}$  and  $k_{\text{cat}}/K_{p\text{NPP}}$  values were obtained at various pH values and saturating concentrations of either  $\text{Mn}^{+2}$  or  $\text{Mg}^{+2}$ . The plot of  $k_{\text{cat}}$  versus pH obtained in  $\text{Mn}^{+2}$  revealed one ionization that must be unprotonated for catalysis and has a  $\text{pK}_a$  value of  $7.00 \pm 0.09$  (Figure 3A). The pH-independent  $k_{\text{cat}}$  value (C) was  $2.21 \pm 0.65$   $\text{s}^{-1}$ . The  $k_{\text{cat}}/K_{p\text{NPP}}$  pH profile obtained in  $\text{Mn}^{+2}$  also exhibited an ionization that must be unprotonated for catalysis, with a  $\text{pK}_a$  value of  $7.18 \pm 0.08$  (Figure 3B). The pH-independent  $k_{\text{cat}}/K_{p\text{NPP}}$  value was  $1,280 \pm 314$   $\text{M}^{-1}\text{s}^{-1}$ . Due to precipitation of  $\text{Mn}^{+2}$  at basic pH values, data could not be collected at pH values higher than 8.5. However, difficulties with precipitation were not encountered with  $\text{Mg}^{+2}$ . This allowed us to measure the  $\text{Mg}^{+2}$ -dependent rates above pH 8.5. The plot of  $k_{\text{cat}}$  versus pH obtained with  $\text{Mg}^{+2}$  revealed an ionization that must be unprotonated for catalysis with a  $\text{pK}_a$  value of  $7.42 \pm 0.09$  (Figure 4A) and a pH-independent value of  $0.11 \pm 0.01$   $\text{s}^{-1}$ . With  $\text{Mg}^{+2}$ , the  $k_{\text{cat}}/K_{p\text{NPP}}$  pH profile revealed a second critical ionization that must be protonated for activity and has a  $\text{pK}_a$  value of  $8.96 \pm 0.12$  (Figure 4B). The pH-independent  $k_{\text{cat}}/K_{p\text{NPP}}$  value was  $20.3 \pm 3.2$   $\text{M}^{-1}\text{s}^{-1}$ .

### *Steady-state Kinetic Analysis.*

Bisubstrate studies were performed to determine the kinetic mechanism of PP2C and to probe the order of substrate binding. The concentration of *p*NPP was varied at fixed concentrations of  $\text{Mn}^{+2}$  and the double-reciprocal plot of  $1/v$  vs.  $1/[p\text{NPP}]$  was constructed for each fixed concentration of  $\text{Mn}^{+2}$  (Figure 5). A series of lines which intersect to the left of the vertical axis and above the horizontal axis were obtained, suggesting a sequential mechanism. In a sequential mechanism, both substrates must bind before catalysis can occur. Thus, PP2C forms a ternary-complex with metal and the phosphomonoester substrate prior to catalysis.

To determine the order of substrate binding and product release, product inhibition studies were performed. The concentration of *p*NPP was varied at fixed levels of  $\text{P}_i$  and saturating levels of  $\text{Mg}^{+2}$ . The double-reciprocal plot revealed a series of lines which intersect at the vertical axis, demonstrating that the inhibition is competitive (Figure 6A). The inhibition constant  $K_{is}$  was determined to be  $0.67 \pm 0.05$  mM. The concentration of  $\text{Mg}^{+2}$  was varied at fixed levels of  $\text{P}_i$  and saturating levels of *p*NPP. A series of parallel lines was obtained in the double-reciprocal plot indicating that  $\text{P}_i$  behaves as an uncompetitive inhibitor with respect to  $\text{Mg}^{+2}$  (Figure 6B). The  $K_{ii}$  value was determined to be  $3.61 \pm 0.16$  mM.

To determine the nature of the rate limiting step during PP2C catalysis, several phosphomonoester substrates with different leaving group  $\text{pK}_a$  values were analyzed. A Brönsted plot of  $\log k_{\text{cat}}$  versus  $\text{pK}_a$  of leaving group was obtained at pH 7.0 and at pH 8.5. At pH 7.0, a  $\beta$  of  $-0.32 \pm 0.03$  (Figure 8) was determined, indicating that chemistry is at least partially rate limiting. A  $\beta$  value of  $0.03 \pm 0.02$  was calculated at pH 8.5 suggesting that chemistry does not contribute to the rate limiting step at this pH. The similar  $k_{\text{cat}}$  values obtained at pH 8.5 for these distinct substrates suggest that they share a common rate limiting step which is independent of the nature of the substrate and the

released alcohol product. The rates obtained with DiFUMBP are identical at pH 7.0 and 8.5, suggesting that the rate limiting step is the same at both pH values and that chemistry does not contribute to the turnover rate with this substrate. With a leaving group  $pK_a$  of 4.6, DiFUMBP does not fall on the Brönsted plot at pH 7. Instead, there appears to be a break in the plot when the  $pK_a$  of the leaving group is less than 7. The Brönsted analysis indicated that the turnover rate of DiFUMBP will not exceed this common slow step, even when chemistry is made very fast with good leaving groups. The point at which the two Brönsted plots cross (Figure 7), appears to represent a transition in the rate limiting step as a function of pH and the  $pK_a$  of the leaving group. Collectively, these data suggest that the common physical release of  $P_i$  may limit the rate of turnover when the rate of chemistry is fast.

#### *Pre-steady-state Kinetics.*

Product inhibition studies revealed that *p*NP is released prior to  $P_i$ . Leaving group dependence studies suggested that at pH 8.5 phosphate release may be the common slow step among the various substrates. If *p*NP release occurs fast relative to a later step, a pre-steady-state “burst” of product should be detectable at pH 8.5. The product *p*NP was a poor inhibitor making  $K_i$  determination difficult; a  $K_i$  value greater than 7 mM was estimated for *p*NP, suggesting that its release from enzyme is rapid and will not contribute to the rate-determining step. At lower pH values and with poorer leaving groups, chemistry is rate limiting, and therefore, we would predict that exponential alcohol product “bursts” would not be observed. On the other hand, if chemistry is fast relative to  $P_i$  release, a burst of *p*NP would be expected according to this mechanism. Using a stopped-flow spectrophotometer, the rapid reaction of PP2C with substrate was followed by measuring the formation of *p*NP and 6,8-difluoro-4-methylumbelliferyl from the substrates *p*NPP and DiFUMBP, respectively. These experiments revealed an exponential product burst at pH 8.5, followed by a slower linear rate (Figure 8A). The amplitude of the

observed burst was proportional to the enzyme concentration (Figure 8B). The burst phase yielded first order rate constants between 20-200 s<sup>-1</sup>, while the linear phase corresponded to the steady-state initial velocity. Burst kinetics were not observed with *p*NPP at pH 7.0, consistent with rate limiting chemistry.

#### *Phospho-peptide Substrate Specificity.*

Several phosphorylated peptides were analyzed to explore PP2C's substrate specificity. The  $k_{\text{cat}}$  and  $k_{\text{cat}}/K_m$  values were determined for a variety of physiologically relevant peptide substrates and are listed in Table II. The  $k_{\text{cat}}$  values were obtained at pH 7.0 and found to range from 0.05 to 0.35 s<sup>-1</sup> compared to 1.02 s<sup>-1</sup> with *p*NPP. Given the  $\text{pK}_a$  for serine/threonine residues, these  $k_{\text{cat}}$  values are 15 to 100-fold faster than the Brönsted plot obtained at pH 7.0 would predict, suggesting that properties intrinsic to the peptide are important for increasing the rate of chemistry at physiological pH values. At pH 8.5, the  $k_{\text{cat}}$  value obtained for the phospho-peptide was similar to the  $k_{\text{cat}}$  obtained for the other substrates at this pH, indicating that dephosphorylation of the peptide is restricted by the same rate limiting step. The  $k_{\text{cat}}/K_m$  values for the peptides approached a 90-fold greater value than that for *p*NPP. Thus, the specificity constants revealed that PP2C prefers peptide substrates over the more rapidly hydrolyzed ( $k_{\text{cat}}$ ) artificial substrates at physiological pH values. The  $k_{\text{cat}}/K_m$  values of the peptides ranged from 3,200 to 75,000 M<sup>-1</sup>s<sup>-1</sup> demonstrating that PP2C discriminates between different peptide substrates. No detectable activity was observed against the tyrosine-phosphorylated peptide KIGEGT(pY)GVVYK, supporting the identification of PP2C as a serine/threonine specific phosphatase.

## Discussion

### *Catalytic Mechanism of PP2C.*

Bisubstrate steady-state kinetics were combined with product inhibition studies to determine the kinetic mechanism of PP2C. The bisubstrate studies revealed a sequential mechanism where both metal cations and phosphorylated substrate must bind prior to catalysis. The product inhibition studies indicated the order of substrate binding and product release. Product  $P_i$  is a competitive inhibitor against  $pNPP$ , suggesting that product and substrate bind the same enzyme form. Product  $P_i$  is an uncompetitive inhibitor with respect to the metal ions, suggesting that  $P_i$  can only bind to the metal-bound form of the enzyme. Thus, if  $P_i$  and  $pNPP$  bind to the same enzyme form and  $P_i$  only binds to the metal-bound form, it follows that the metal ions bind prior to  $pNPP$  and that  $P_i$  is the last product to be released. In summary, our kinetic analysis of PP2C suggests an ordered sequential mechanism where PP2C binds  $Mg^{+2}$  before  $pNPP$ . The products are released in the order  $pNP$  and then  $P_i$  (Scheme 1).

The pH profiles have revealed an enzyme ionization that must be unprotonated for catalysis ( $pK_a$  7) and an additional ionization that must be protonated for substrate binding ( $pK_a$  9). Based on the X-ray structure of PP2C (10), the identity of these important ionizable groups is somewhat ambiguous. Das *et al.* (10) reported the presence of 5 carboxylic acid residues (Asp-38, -60, -239, -282, and Glu-37) involved in metal binding and an arginine (Arg-33) involved in phosphate binding. No amino acid side-chain nucleophile was apparent from the structure. Das *et al.* (10) proposed that a water molecule bridged between the two metals is the nucleophile which attacks the phosphoester in a single chemical step. The ionizable group that must be unprotonated with a  $pK_a = 7.0$  is consistent with a metal-bound water molecule, acting as the nucleophile (10). There are several examples of metallohydrolases where the proposed nucleophile is an activated



water molecule with a  $pK_a \sim 7$  (25) (26). Although the X-ray structure does not suggest the identity of the protonated group with  $pK_a$  value of 9, this ionization could result from a structurally important group (perhaps tyrosine, cysteine or lysine) that must be protonated for substrate binding. It is unlikely to be a cysteine residue, as iodoacetate modification of PP2C does not affect activity (data not shown). It is worthy to note that the X-ray structure was determined at pH 5. Under these conditions the enzyme is incorrectly protonated and therefore the structure is that of the inactive form of PP2C. It is quite possible that significant structural changes will accompany this shift from inactive enzyme at pH 5 to active enzyme above pH 7. Future mutational studies coupled to a detailed kinetic analysis should provide these answers.

The Brönsted plots indicated that increasing the pH from 7.0 to 8.5 results in a change in the rate limiting step for substrates having  $pK_a$  values greater than about 7. At pH 7.0, chemistry is rate limiting and at pH 8.5 a step common to all substrates becomes rate limiting. The rate of turnover for substrates with  $pK_a$  values below 7 does not significantly increase with increasing pH. For instance, DiFUMBP ( $pK_a$  4.9) clearly does not fit on the Brönsted plot obtained at pH 7.0, suggesting that chemistry is not rate limiting for this substrate at either pH value. The fact that the rate for DiFUMBP hydrolysis is not accelerated by increasing pH, is consistent with a mechanism where a step independent of leaving group  $pK_a$  and common to all substrates is rate limiting at pH 8.5. That same step becomes rate limiting at pH 7.0 as the leaving group  $pK_a$  decreases (i.e. chemistry is fast). Since chemistry is fast for substrates with low  $pK_a$  values, the turnover rates are governed by the same slow step at both pH 7.0 and 8.5 ( $k_{cat} \sim 1.5 \text{ s}^{-1}$ ). Consistent with the minimal kinetic mechanism proposed in Scheme 1, the physical release of phosphate would be a common step that is independent of the nature of the phosphomonoester and the alcohol product.

To explore the possibility that phosphate release was rate limiting at pH 8.5, pre-steady-state kinetic experiments were performed to determine if an exponential burst of the

alcohol product could be detected prior to the build-up of the steady-state rate. The Brönsted plots suggest that at pH 8.5, phosphate release may be the rate limiting step. These data also indicated that as the leaving group  $pK_a$  decreases, chemistry becomes less rate limiting, or phosphate release becomes more rate limiting. This suggested that product bursts could be observed at pH 8.5 with substrates which have lower leaving group  $pK_a$  values, such as *p*NPP and DiFUMBP. The detection of a pre-steady-state burst requires that the release of the chromophoric product (*p*NP and DiFUMB) occurs before the rate limiting step in the reaction. The product inhibition studies suggested that phosphate release is the last kinetic step. If phosphate release is the rate limiting step, a burst of product (*p*NP and DiFUMB) would be detectable upon rapid mixing of enzyme and substrate. The detection of product bursts (Figure 8) whose amplitude correlates with the enzyme concentration is in excellent agreement with this kinetic model.

Although X-ray studies did not reveal a nucleophilic residue (10), we cannot rule out the possibility that PP2C forms a phosphoenzyme intermediate. Both the pre-steady-state and steady-state data are also fully consistent with this mechanism. In this model, formation of the intermediate would limit turnover at low pH, while at high pH intermediate hydrolysis would be rate-determining. The phosphoenzyme intermediate mechanism would be akin to that utilized by the protein tyrosine phosphatases (27). The fact that we were unable to trap a phosphoenzyme intermediate with a variety of peptide substrates at pH 8.5, argues against the involvement of a side-chain nucleophile, and as we have proposed, suggests that the slow step at pH 8.5 involves the physical release of phosphate after the rapid attack of the metal bound water molecule.

#### *Metal-Dependence.*

The metal ions  $Mg^{+2}$  and  $Mn^{+2}$  were previously shown to activate putative PP2C enzymes. The results reported here reveal that PP2C is most active with  $Fe^{+2}$ , as determined by comparing  $k_{cat}$  and  $k_{cat}/K_{metal}$  values obtained with various metal cations. The

metal dependence is of interest since the physiological metals ions of PP2C are not known. A comparison of  $k_{\text{cat}}/K_{\text{metal}}$  values suggests that  $\text{Fe}^{+2}$  is preferred over all other metal ions analyzed. In fact, the  $k_{\text{cat}}/K_{\text{metal}}$  for  $\text{Fe}^{+2}$  was determined to be 1,800 fold greater than the  $k_{\text{cat}}/K_{\text{metal}}$  obtained with  $\text{Mg}^{+2}$ . This was surprising considering that PP2C was initially defined by its  $\text{Mg}^{+2}$ -dependence (28) and that there were no previous reports of PP2C  $\text{Fe}^{+2}$ -dependent activity.

The importance of the iron oxidation state appears to be similar to that seen with the diiron proteins, ribonucleotide reductase and purple acid phosphatase. Ribonucleotide reductase has been shown to only bind  $\text{Fe}^{+2}$  (29). The oxidation of one of the  $\text{Fe}^{+2}$  ions in ribonucleotide reductase is required for the activation of this enzyme. The active form of purple acid phosphatase is thought to be the mixed-valence state with an  $\text{Fe}^{+3}\text{-Fe}^{+2}$  center. This mixed valence state can be mimicked by an  $\text{Fe}^{+3}\text{-Zn}^{+2}$  center (30) in oxidized purple acid phosphatase. Studies with the PPP calcineurin revealed that the active site of the native enzyme consists of one  $\text{Zn}^{+2}$  and one  $\text{Fe}^{+3}$  ion (31). Calcineurin can be reconstituted with Fe and the active form has been shown to consist of an  $\text{Fe}^{+3}\text{-Fe}^{+2}$  containing active site (32). Our experiments demonstrating the correlation between decreased activity and the oxidation of  $\text{Fe}^{+2}$ , indicates that the dinuclear site of active PP2C consists of at least one  $\text{Fe}^{+2}$  cation. The metal-dependent activity of PP2C suggests that both the nature of the metal and its valence state will play a key role in regulating the cellular activity of PP2C.

### *Substrate Specificity.*

Although artificial substrates yielded  $k_{\text{cat}}$  values higher than those obtained with several phosphorylated peptides (Table 2), the  $k_{\text{cat}}/K_{\text{m}}$  values clearly demonstrated that phospho-peptides are greatly preferred over the artificial substrates examined. The  $k_{\text{cat}}/K_{\text{m}}$  values are more useful for analyzing the substrate specificity, since the  $k_{\text{cat}}/K_{\text{m}}$  constant reflects both binding and catalysis, whereas  $k_{\text{cat}}$  does not reflect binding affinity. The  $k_{\text{cat}}/K_{\text{m}}$  for the Cdc2 peptide KIGEG(pT)(pY)GVVYK was 85-fold greater than the  $k_{\text{cat}}/K_{\text{m}}$

value for *p*NPP. The peptide DDENle(pT)G(pY)VATR, corresponding to the activation lip of PP2C's authentic *in vivo* substrate p38 (6), was also found to be a far better substrate than *p*NPP, with an 18-fold greater  $k_{\text{cat}}/K_m$  value. It is interesting to note that diphosphorylated peptides (Table 2) appear to be much better substrates, than singly threonine-phosphorylated peptides. This is a significant observation since the proposed substrates MKK6, SEK 1 and p38 (6) are diphosphorylated on neighboring residues. Collectively, this may suggest that a large component of PP2C's substrate specificity lies within the ability to recognize and bind the diphosphorylated "active" form of these physiological substrates. By analogy, the dual-specificity protein tyrosine phosphatases (DS-PTPs) are believed to specifically recognize and dephosphorylate the diphosphorylated forms of the MAP kinases (19)(33). With the DS-PTPs, both phospho-residues can be hydrolyzed, although a few DS-PTPs will only catalyzed hydrolysis of phosphotyrosine in the context of the diphosphorylated species (19)(33).

## Tables

**Table I. Human PP2C $\alpha$  Metal Dependence**

Metal ion	$k_{cat}$ s <sup>-1</sup>	$K_{metal}$ mM	$k_{cat}/K_{metal}$ M <sup>-1</sup> s <sup>-1</sup>
Mn <sup>2+</sup>	0.96 +/- 0.01	1.42 +/- 0.08	670.0 +/- 30.0
Mg <sup>2+</sup>	0.038 +/- 0.002	20.6 +/- 1.7	1.80 +/- 0.10
Fe <sup>2+</sup>	21.5 +/- 3.3	6.56 +/- 2.26	3290.0 +/- 660.0
Co <sup>2+</sup>	0.30 +/- 0.05	7.2 +/- 2.4	42.0 +/- 7.0
Cu <sup>2+</sup>	ND*	>20	3.30 +/- 0.30
Ni <sup>2+</sup>	0.006 +/- 0.001	11.9 +/- 6.1	0.30 +/- 0.04
Zn <sup>2+</sup>	~0	12.0 +/- 1.8	$K_i$ $\mu$ M
Ca <sup>2+</sup>	~0	4.45 +/- 0.54	$K_i$ mM

\*ND: Not Determined. Unable to saturate due to precipitation at higher [Cu<sup>2+</sup>].

All assays performed in Tris/Tris-Bis/Acetate buffer pH 7.0, 25 °C at 20 mM pNPP.

$K_i$  values determined with Mn<sup>2+</sup> as metal substrate.

**Table II. Substrate Specificity of PP2C $\alpha$** 

Substrate	$k_{cat}$ s <sup>-1</sup>	$K_m$ mM	$k_{cat}/K_m$ M <sup>-1</sup> s <sup>-1</sup>
<i>p</i> NPP	1.02 +/- 0.01	1.18 +/- 0.03	859.0 +/- 15.9
KIGEG(pT)(pY)GVVYK Cdc2	0.35 +/- 0.04	0.005 +/- 0.001	75,000 +/- 18,000
KIGEGT(pY)GVVYK Cdc2	~0	~0	~0
DDENle(pT)G(pY)VATR p38	0.23 +/- 0.01	0.015 +/- 0.002	15,300 +/- 1,500
FNleNle(pY)P(pT)VVTR $\Psi$ JNK-1	0.09 +/- 0.01	0.006 +/- 0.003	14,800 +/- 4,800
GIPIRVY(pT)HEV Cdc2	0.30 +/- 0.04	0.09 +/- 0.05	3,200 +/- 1,200

Assays performed in Tris/Tris-Bis/Acetate buffer pH 7.0, 10 mM Mn<sup>2+</sup>.

The  $k_{cat}$  values are based on P<sub>i</sub> released.

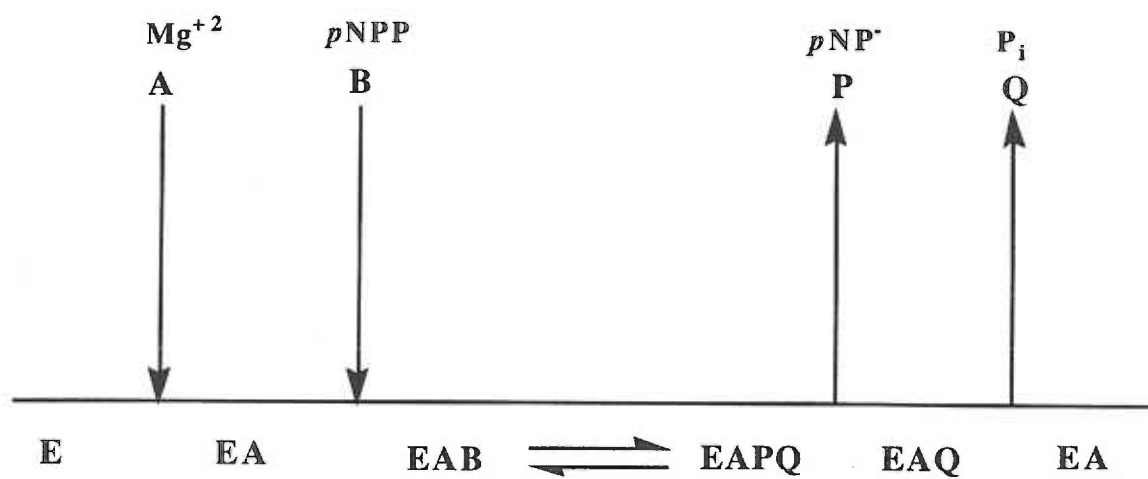
$\Psi$ : Variations of native sequence, FNleNle(pT)P(pY)VVTR.

**Table III. PP2C $\alpha$  pH Dependence**

Profile	Metal Ion	C	pK <sub>a1</sub>	pK <sub>a2</sub>
k <sub>cat</sub>	Mn <sup>+2</sup>	2.21 $\pm$ 0.65 s <sup>-1</sup>	7.00 $\pm$ 0.09	--
k <sub>cat</sub> /K <sub>pNPP</sub>	Mn <sup>+2</sup>	1,280 $\pm$ 314 M <sup>-1</sup> s <sup>-1</sup>	7.18 $\pm$ 0.08	--
k <sub>cat</sub>	Mg <sup>+2</sup>	0.11 $\pm$ 0.01 s <sup>-1</sup>	7.42 $\pm$ 0.09	--
k <sub>cat</sub> /K <sub>pNPP</sub>	Mg <sup>+2</sup>	20.3 $\pm$ 3.2 M <sup>-1</sup> s <sup>-1</sup>	7.23 $\pm$ 0.12	8.96 $\pm$ 0.12

Assays performed in Tris/Tris-Bis/Acetate buffer, 25°C. Rates were monitored by measuring *p*NP formation spectrophotometrically at 410 nm. Profiles for Mn<sup>+2</sup> were determined between pH 5 and 8.5. Precipitation prevented obtaining data at higher pH values. Profiles for Mg<sup>+2</sup> were determined between pH 5 and 10.3. C is the pH-independent value of either k<sub>cat</sub> or k<sub>cat</sub>/K<sub>m</sub>.

## Scheme 1





## Figures

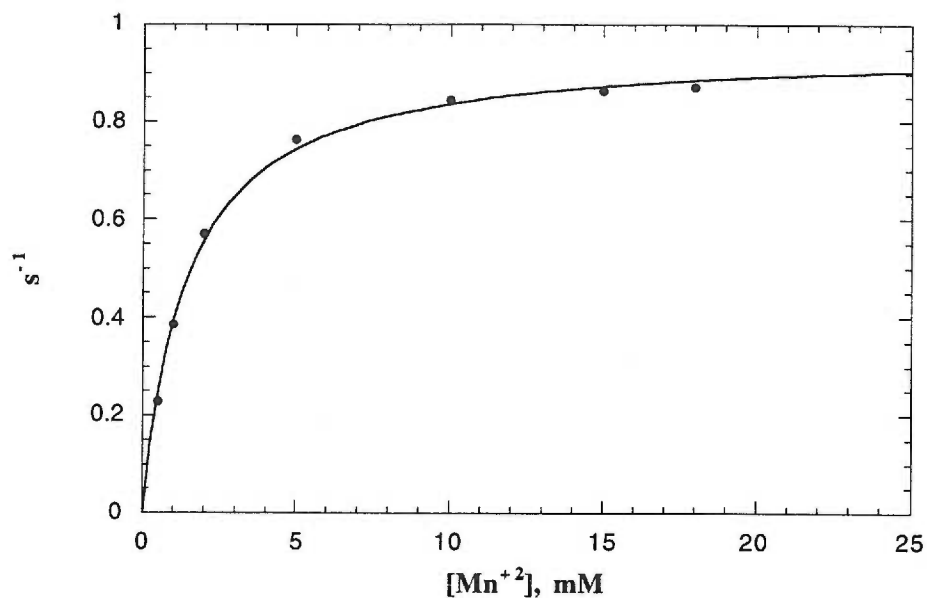


**Figure 1. Saturation kinetics of PP2C with Mn<sup>2+</sup>.**

The saturation of PP2C activity with increasing concentrations of Mn<sup>2+</sup>. The Mn<sup>2+</sup> concentration was varied at saturating *p*NPP and the rates were determined by measuring the production of *p*NP at 410 nm. The data were fitted to the Michaelis-Menten equation  $v = (k_{cat} S / (K_m + S))$ . Assays performed in Tris/Bis-Tris/Acetate buffer pH 7.0, 25°C.

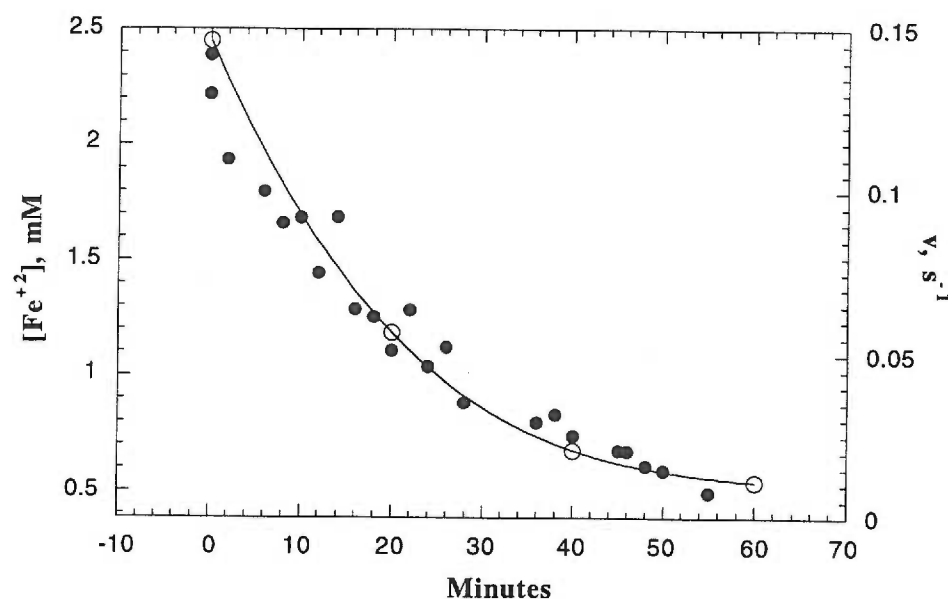


**Figure 2. Oxidation of Fe<sup>2+</sup> correlates with loss in PP2C activity.**

The loss of Fe<sup>2+</sup> with time was detected with the Fe<sup>2+</sup> specific chromophore, Ferrozine.

The loss in [Fe<sup>2+</sup>] correlates with the loss of PP2C activity. PP2C activity was monitored using the continuous assay described in Experimental Procedures. Assays performed in Tris/Bis-Tris/Acetate buffer pH 7.0, 25°C. The concentration of Fe<sup>2+</sup> is represented by ●, and the remaining PP2C activity is represented by ○.

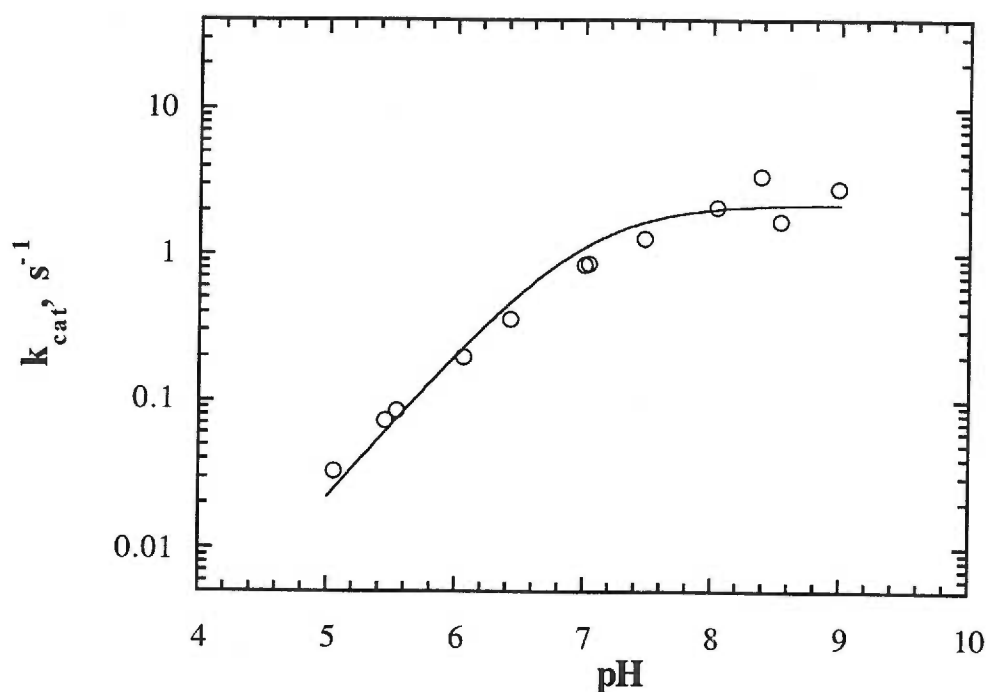


**Figure 3 A. Effect of pH on the  $k_{cat}$  parameter at saturating  $Mn^{+2}$ .** Initial velocities were determined at various  $pNPP$  concentrations in saturating levels of  $Mn^{+2}$  at the indicated pH values. The  $k_{cat}$  values were determined by fitting the data to the Michaelis-Menten equation  $v = (V_{max} \cdot S) / (K_m + S)$ , as described in Experimental Procedures. The pH data were fitted to the equation  $v = C / (1 + H/K_a)$ . The  $pK_a$  value was  $7.00 \pm 0.09$ . The assay conditions were 0.1 M acetate/0.05 M Tris/0.05 M Bis-Tris at 25 °C in 10 mM  $Mn^{+2}$ .

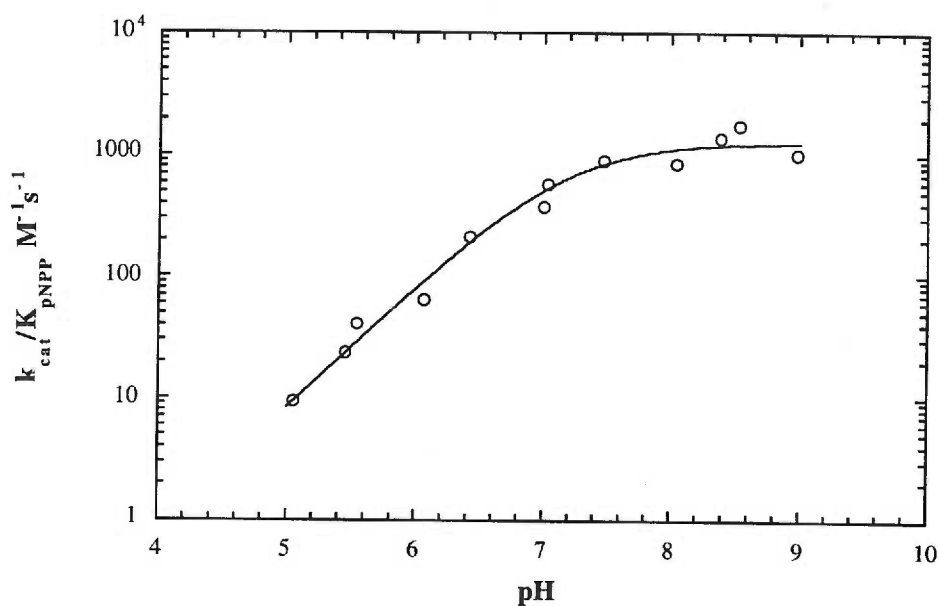


**Figure 3 B. Effect of pH on the  $k_{cat}/K_m$  parameter at saturating  $\text{Mn}^{+2}$ .** Initial velocities were determined at various  $p\text{NPP}$  concentrations in saturating levels of  $\text{Mn}^{+2}$  at the indicated pH values. The  $k_{cat}/K_m$  values were determined by fitting the data to the Michaelis-Menten equation  $v = (V_{max} \cdot S) / (K_m + S)$ , as described in Experimental Procedures. The pH data were fitted to the equation  $v = C / (1 + H/K_a)$ . The  $pK_a$  value was  $7.18 \pm 0.08$ . The assay conditions were 0.1 M acetate/0.05 M Tris/0.05 M Bis-Tris at 25 °C in 10 mM  $\text{Mn}^{+2}$ .

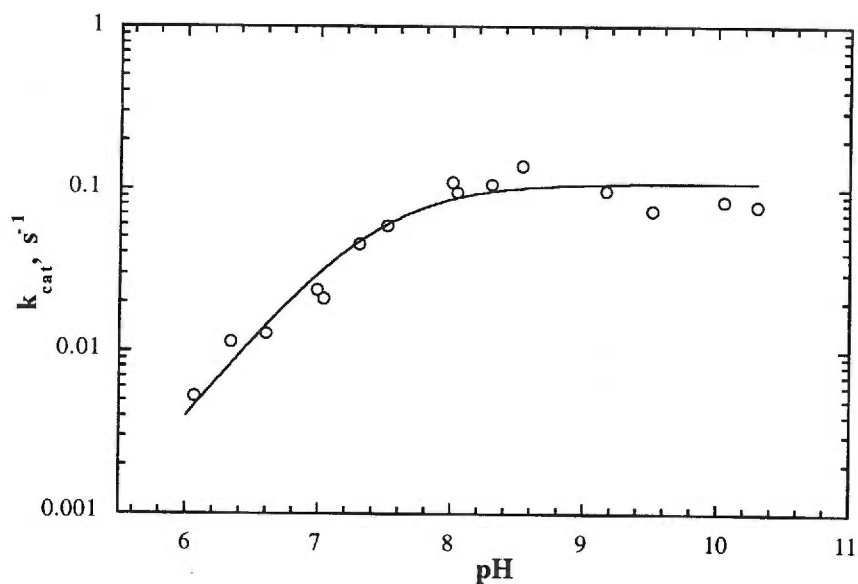


**Figure 4 A. Effect of pH on the  $k_{cat}$  parameter at saturating  $Mg^{+2}$ .** The  $k_{cat}$  value were determined by varying the concentration of *p*NPP in saturating  $Mg^{+2}$  at the indicated pH values and fitting the data to the Michaelis-Menten equation. The pH data were fitted using the equation  $v = C / (1 + H/K_a)$  and yielded a  $pK_a$  value of  $7.42 \pm 0.09$ . The assay conditions were 0.1 M acetate/0.05 M Tris/0.05 M Bis-Tris at 25 °C in saturating  $Mg^{+2}$  (40 mM).

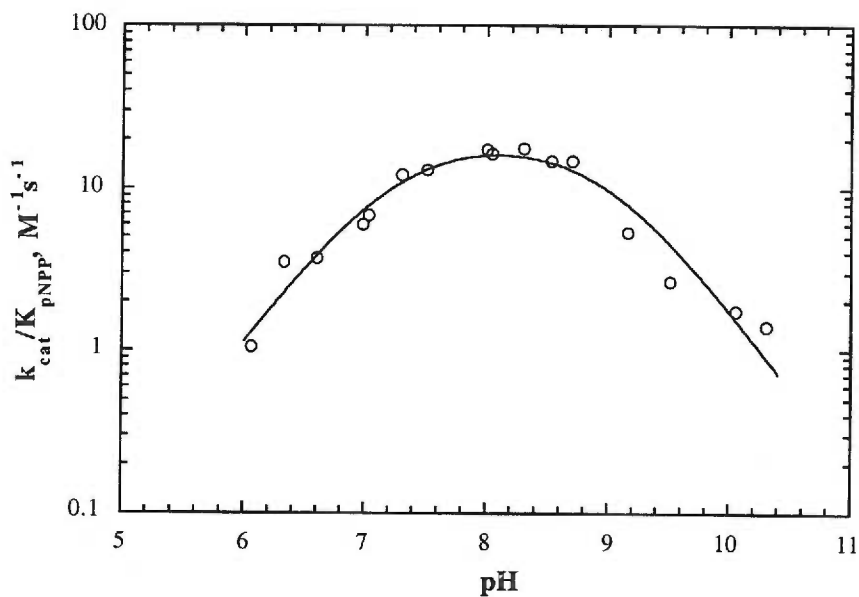


**Figure 4B.** Effect of pH on the  $k_{cat}/K_{pNPP}$  parameter at saturating  $Mg^{+2}$ . The  $k_{cat}/K_m$  values were determined by varying the concentration of  $pNPP$  in saturating  $Mg^{+2}$  at the indicated pH values and fitting the data to the Michaelis-Menten equation. The pH data for  $k_{cat}/K_m$  (4B) was fitted using the equation  $v = C / (1 + H/K_a + K_b/H)$ , yielding  $pK_a$  values of  $7.23 \pm 0.12$  and  $8.96 \pm 0.12$ . The assay conditions were 0.1 M acetate/0.05 M Tris/0.05 M Bis-Tris at 25 °C in saturating  $Mg^{+2}$  (40 mM).

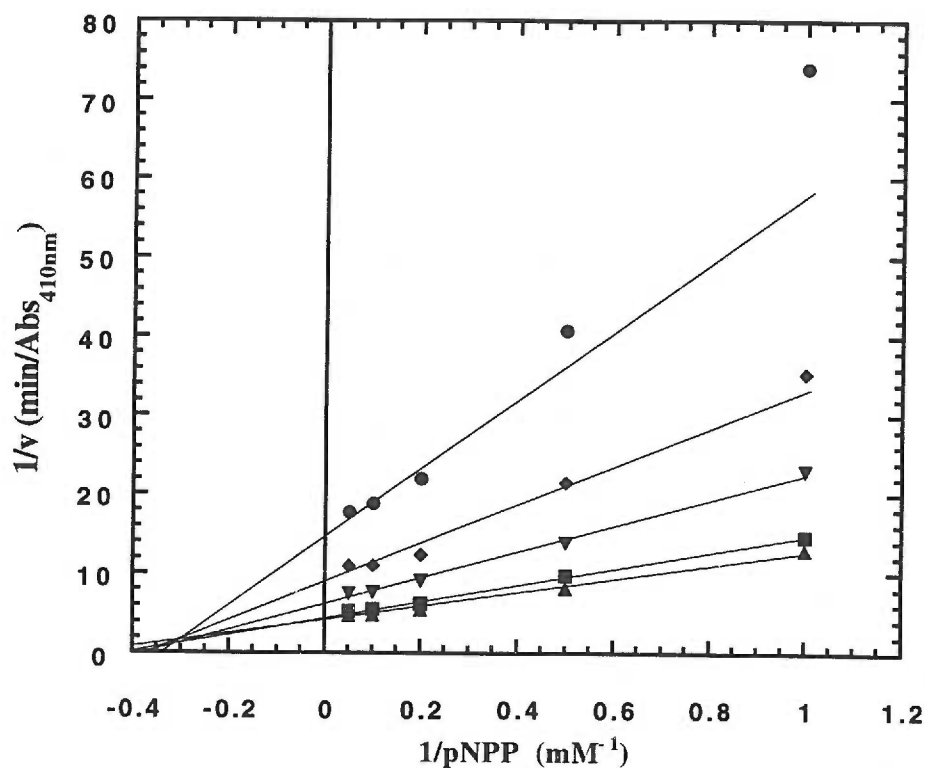


**Figure 5.** Ternary-complex mechanism of PP2C $\alpha$ .

Double-reciprocal plots of  $1/\text{velocity}$  vs.  $1/[p\text{NPP}]$  at several fixed concentrations of metal cation ( $\text{Mn}^{+2}$ ). Data were fitted to the equation for a sequential mechanism as described in Experimental Procedures. Continuous assays were utilized to monitor  $p\text{NPP}$  hydrolysis at pH 7.0, 25 °C. The  $\text{Mn}^{+2}$  concentrations were  $\bullet$  0.5 mM,  $\blacklozenge$  1.0 mM,  $\blacktriangledown$  2.0 mM,  $\blacksquare$  5.0 mM, and  $\blacktriangle$  10.0 mM.

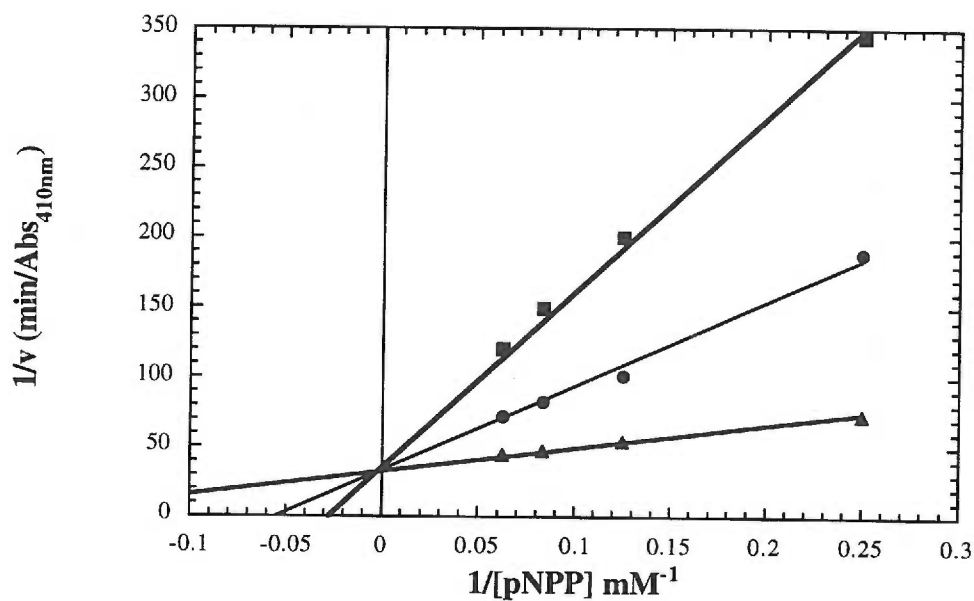


**Figure 6A. Phosphate inhibition of PP2C at varied  $pNPP$ .**

(A) With  $pNPP$  as the varied substrate at saturating  $[Mn^{+2}]$ , double-reciprocal plots for phosphate inhibition demonstrate that phosphate is a competitive inhibitor with respect to  $pNPP$ . A  $K_{is} = 0.67 \pm 0.05 \text{ mM}$  was determined as described in Experimental Procedures. The  $P_i$  concentrations were ■ 5.0 mM, ● 2.0 mM and ▲ 0 mM.



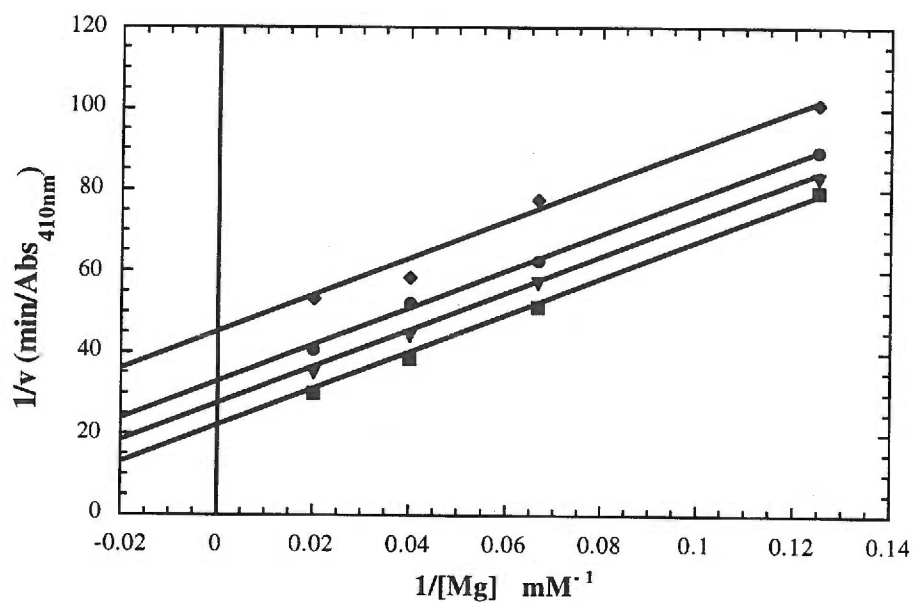


**Figure 6B. Phosphate inhibition of PP2C at varied metal.** Phosphate inhibition analysis at varied metal concentrations in saturating *p*NPP revealed uncompetitive inhibition with respect to the metal. A  $K_{ii} = 3.61 \pm 0.16$  mM was determined as described in Experimental Procedures. The  $P_i$  concentrations were  $\blacklozenge$  4.0 mM,  $\bullet$  2.0 mM,  $\blacktriangledown$  1.0 mM and  $\blacksquare$  0 mM.

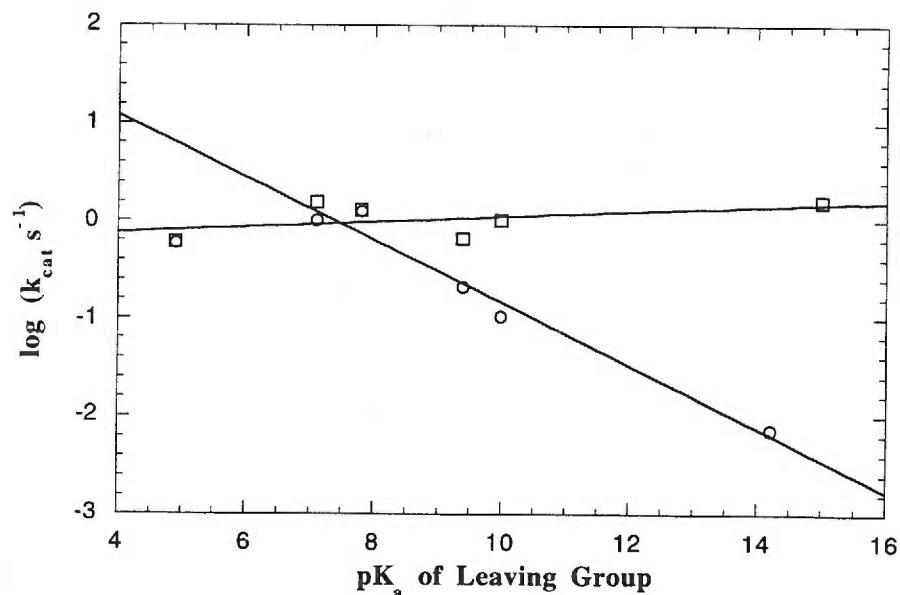


**Figure 7.** Effect of leaving group  $pK_a$  value on the  $k_{cat}$ . Substrates DiFUMBP ( $pK_a = 4.9$ ),  $pNPP$  (7.1), 4-methylumbelliferyl phosphate (7.8),  $\beta$ -naphthyl phosphate (9.38) and phenyl phosphate (9.99), phosphoserine (14.2), and the phosphothreonine containing peptide, GIPRVY(pT)HEV (15) were analyzed using the phosphate detection assay at pH 7.0 (circles) and 8.5 (squares). Linear least-squares fitting of Brønsted plots yielded slopes ( $\beta$ ) of  $-0.32 \pm 0.03$  at pH 7.0 and  $0.03 \pm 0.02$  at pH 8.5. The  $k_{cat}$  obtained at pH 7.0 for DiFUMBP was not included for the calculation of  $\beta$  at pH 7.0 (see Results section). The assay conditions were 0.1 M acetate/0.05 M Tris/0.05 M Bis-Tris at 25 °C in 10 mM  $Mn^{+2}$ .

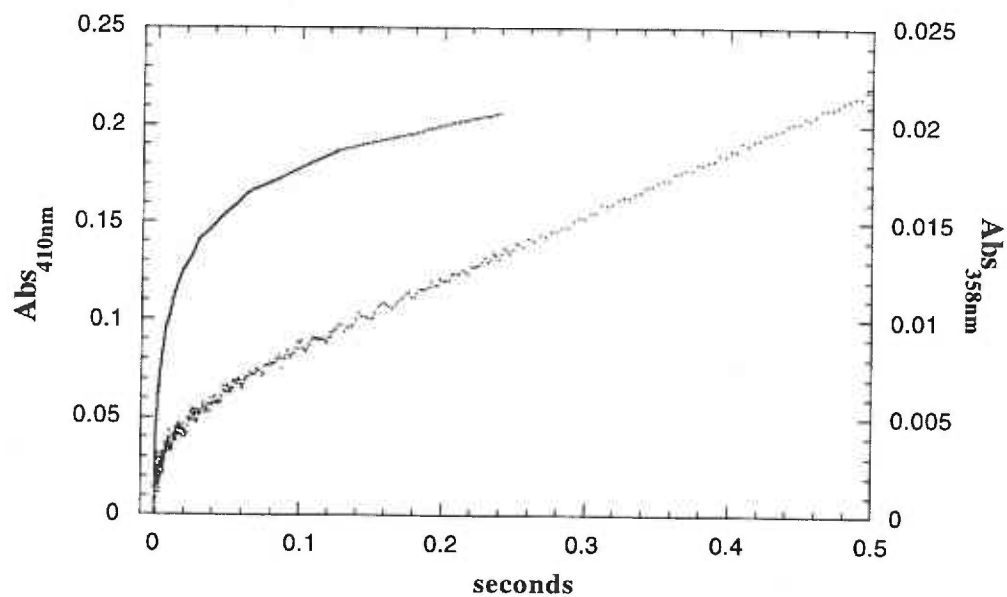


**Figure 8A. Pre-steady state analysis reveals product “burst.”** Stopped-flow traces of product formation after rapid mixing of PP2C and *p*NPP (top trace) or DiFUMBP (bottom trace). Conditions: 0.1 M acetate/0.05 M Tris/0.05 M Bis-Tris pH 8.5 and 10 mM  $\text{Mn}^{+2}$ . The final concentration of *p*NPP was 10 mM; the final concentration DiFUMBP was 5 mM.

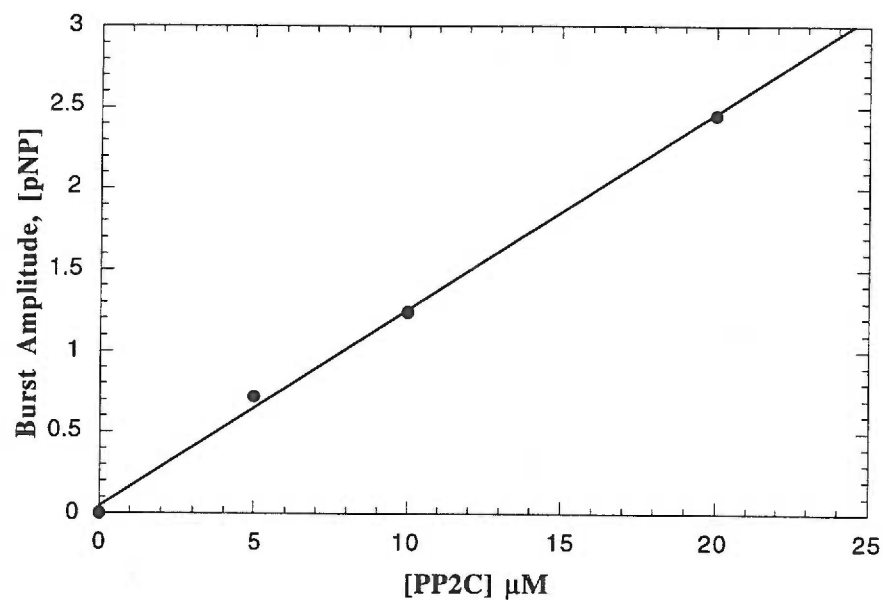


**Figure 8B. Burst amplitude is dependent on enzyme concentration.** Each point is an average of the data from three traces obtained at the indicated enzyme concentrations. Data were fitted using linear least-squares. Conditions: 0.1 M acetate/0.05 M Tris/0.05 M Bis-Tris pH 8.5 and 10 mM  $\text{Mn}^{+2}$  at 10 mM *p*NPP.

## SUMMARY AND CONCLUSIONS

The PPM family of Ser/Thr Protein Phosphatases have recently been shown to downregulate the stress response pathways in eukaryotes. Within the stress pathway, key signaling kinases, which are activated by protein phosphorylation, have been proposed as the *in vivo* substrates of PP2C, the prototypical member of the PPM family. Although it is known that these phosphatases require metal cations for activity, the molecular details of these important reactions have not been established. Therefore, here we report a detailed biochemical study to elucidate the kinetic and chemical mechanism of PP2C $\alpha$ . Steady-state kinetic and product inhibition studies revealed that PP2C $\alpha$  employs an ordered sequential mechanism, where the metal cations bind before phosphorylated substrate, and phosphate is the last product to be released. The metal-dependent activity of PP2C (as reflected in  $k_{\text{cat}}$  and  $k_{\text{cat}}/K_{\text{m}}$ ), indicated that  $\text{Fe}^{+2}$  was 1000-fold better than  $\text{Mg}^{+2}$ . The pH rate profiles revealed two ionizations critical for catalytic activity. An enzyme ionization with a  $\text{pK}_{\text{a}}$  value of 7 must be unprotonated for catalysis and an enzyme ionization with a  $\text{pK}_{\text{a}}$  of 9 must be protonated for substrate binding. Brönsted analysis of substrate leaving group  $\text{pK}_{\text{a}}$  indicated that phosphomonoester hydrolysis is rate limiting at pH 7.0, but not at pH 8.5 where a common step independent of the nature of the substrate and alcohol product limits turnover ( $k_{\text{cat}}$ ). Rapid reaction kinetics between phosphomonoester and PP2C yielded exponential “bursts” of product formation, consistent with phosphate release being the slow catalytic step at pH 8.5. Dephosphorylation of synthetic phosphopeptides corresponding to several protein kinases revealed that PP2C displays a strong preference for diphosphorylated peptides in which the phosphorylated residues are in close proximity.

## REFERENCES

1. Barford, D. (1996) *Trends Biochem Sci* **21**(11), 407-12
2. Waskiewicz, A. J., and Cooper, J. A. (1995) *Curr Opin Cell Biol* **7**(6), 798-805
3. Kyriakis, J. M., and Avruch, J. (1996) *J Biol Chem* **271**(40), 24313-6
4. Raingeaud, J., Gupta, S., Rogers, J. S., Dickens, M., Han, J., Ulevitch, R. J., and Davis, R. J. (1995) *J Biol Chem* **270**(13), 7420-6
5. Meskiene, I., Bogre, L., Glaser, W., Balog, J., Brandstotter, M., Zwerger, K., Ammerer, G., and Hirt, H. (1998) *Proc Natl Acad Sci U S A* **95**(4), 1938-43
6. Takekawa, M., Maeda, T., and Saito, H. (1998) *Embo J* **17**(16), 4744-52
7. Hanada, M., Kobayashi, T., Ohnishi, M., Ikeda, S., Wang, H., Katsura, K., Yanagawa, Y., Hiraga, A., Kanamaru, R., and Tamura, S. (1998) *FEBS Lett* **437**(3), 172-6
8. Shiozaki, K., and Russell, P. (1995) *Embo J* **14**(3), 492-502
9. Gaits, F., Shiozaki, K., and Russell, P. (1997) *J Biol Chem* **272**(28), 17873-9
10. Das, A. K., Helps, N. R., Cohen, P. T., and Barford, D. (1996) *Embo J* **15**(24), 6798-809
11. Martin, B. L., and Graves, D. J. (1994) *Biochim Biophys Acta* **1206**(1), 136-42
12. Mueller, E. G., Crowder, M. W., Averill, B. A., and Knowles, J. R. (1993) *J. Am. Chem. Soc.* **115**, 2974-2975
13. Vincent, J. B., Crowder, M. W., and Averill, B. A. (1991) *J Biol Chem* **266**(27), 17737-40
14. Denu, J. M., Stuckey, J. A., Saper, M. A., and Dixon, J. E. (1996) *Cell* **87**(3), 361-364
15. Bradshaw, R. A., Cancedda, F., Ericsson, L. H., Neumann, P. A., Piccoli, S. P., Schlesinger, M. J., Shrieffer, K., and Walsh, K. A. (1981) *Proc Natl Acad Sci U S A* **78**(6), 3473-7

16. Ostanin, K., Harms, E. H., Stevis, P. E., Kuciel, R., Zhou, M. M., and Van Etten, R. L. (1992) *J Biol Chem* **267**(32), 22830-6
17. Davies, S. P., Helps, N. R., Cohen, P. T., and Hardie, D. G. (1995) *FEBS Lett.* **377**(3), 421-425
18. Brotherus, J. R., Jacobsen, L., and Jorgensen, P. L. (1983) *Biochim Biophys Acta* **731**(2), 290-303
19. Denu, J. M., Zhou, G., Wu, L., Zhao, R., Yuvaniyama, J., Saper, M. A., and Dixon, J. E. (1995) *J Biol Chem* **270**(8), 3796-3803
20. Kyte, J. (1995) *Mechanism in Protein Chemistry*, Garland Publishing, Inc., New York & London
21. Lee, M. G., and Nurse, P. (1987) *Nature* **327**(6117), 31-5
22. Wilson, K. P., Fitzgibbon, M. J., Caron, P. R., Griffith, J. P., Chen, W., McCaffrey, P. G., Chambers, S. P., and Su, M. S. (1996) *J Biol Chem* **271**(44), 27696-700
23. Gupta, S., Barrett, T., Whitmarsh, A. J., Cavanagh, J., Sluss, H. K., Derijard, B., and Davis, R. J. (1996) *Embo J* **15**(11), 2760-70
24. Pato, M. D., and Kerc, E. (1991) *Mol Cell Biochem* **101**(1), 31-41
25. Pohjanjoki, P., Lahti, R., Goldman, A., and Cooperman, B. S. (1998) *Biochemistry* **37**(7), 1754-61
26. Chen, G., Edwards, T., D'Souza, V. M., and Holz, R. C. (1997) *Biochemistry* **36**(14), 4278-86
27. Denu, J. M., Lohse, D. L., Vijayalakshmi, J., Saper, M. A., and Dixon, J. E. (1996) *Proc Natl Acad Sci U S A* **93**(6), 2493-8
28. Ingebritsen, T. S., and Cohen, P. (1983) *Science* **221**(4608), 331-8
29. Petersson, L., Graslund, A., Ehrenberg, A., Sjoberg, B. M., and Reichard, P. (1980) *J Biol Chem* **255**(14), 6706-12
30. Merckx, M., and Averill, B. A. (1998) *Biochemistry* **37**(32), 11223-31

31. King, M. M., and Huang, C. Y. (1984) *J Biol Chem* **259**(14), 8847-56
32. Yu, L., Golbeck, J., Yao, J., and Rusnak, F. (1997) *Biochemistry* **36**(35), 0727-34
33. Todd, J. L., Tanner, K. G., and Denu, J. M. (1999) *J. Biol. Chem.* **in press**